

- Valls-Solé, J., Pascual-Leone, A., Wassermann, E.M. & Hallett, M. (1992) Human motor evoked responses to paired transcranial magnetic stimuli. *Electroencephalography Clinical Neurophysiology*, **85**, 355–364.
- Walsh, V. & Rushworth, M. (1999) A primer of magnetic stimulation as a tool for neuropsychology. *Neuropsychologia*, **37**, 125–135.
- Zangen, A., Roth, Y., Voller, B. & Hallett, M. (2005) Transcranial magnetic stimulation of deep brain regions: evidence for efficacy of the H-coil. *Clinical Neurophysiology*, **116**, 775–779.
- Zanon, M., Busan, P., Monti, F., Pizzolato, G. & Battaglini, P.P. (2010) Cortical connections between dorsal and ventral visual streams in humans: Evidence by TMS/EEG co-registration. *Brain Topography*, **22**, 307–317.
- Ziemann, U. (2010) TMS in cognitive neuroscience: virtual lesion and beyond. *Cortex*, **46**, 124–127.
- Ziemann, U. & Rothwell, J.C. (2000) I-waves in motor cortex. *Journal of Clinical Neurophysiology*, **17**, 397–405.
- Ziemann, U., Rothwell, J.C. & Ridding, M.C. (1996a) Interaction between intracortical inhibition and facilitation in human motor cortex. *Journal of Physiology*, **496** (Pt 3), 873–881.
- Ziemann, U., Lönneker, S., Steinhoff, B.J. & Paulus, W. (1996b) The effect of lorazepam on the motor cortical excitability in man. *Experimental Brain Research*, **109**, 127–135.
- Ziemann, U., Lönneker, S., Steinhoff, B.J. & Paulus, W. (1996c) Effects of antiepileptic drugs on motor cortex excitability in humans: a transcranial magnetic stimulation study. *Annals of Neurology*, **40**, 367–378.
- Ziemann, U., Ilic, T.V., Pauli, C., Meintzschel, F. & Ruge, D. (2004) Learning modifies subsequent induction of long-term potentiation-like and long-term depression-like plasticity in human motor cortex. *Journal of Neuroscience*, **24**, 1666–1672.
- Ziemann, U., Tergau, F., Wassermann, E.M., Wischer, S., Hildebrandt, J. & Paulus, W. (1998) Demonstration of facilitatory I wave interaction in the human motor cortex by paired transcranial magnetic stimulation. *Journal of Physiology*, **511** (Pt 1), 181–190.
- Ziemann, U., Paulus, W., Nitsche, M.A. et al. (2008) Consensus: motor cortex plasticity protocols. *Brain Stimulation*, **1**, 164–182.

10 Advances in Transcranial Magnetic Stimulation Technology

Angel V. Peterchev, Zhi-De Deng and Stefan M. Goetz

Department of Psychiatry and Behavioral Sciences, Duke University School of Medicine, Durham, NC, USA

Introduction

The importance of transcranial magnetic stimulation (TMS) as a research and clinical tool depends on the capabilities of the underlying technology. A TMS device consists of two key components: a pulse source and a stimulation coil. The pulse source is typically housed in a desktop box that is sometimes mounted on a cart. The pulse source is connected to the coil through a high-voltage, high-current cable. The coil may be of various shapes and is placed on the subject's head. The pulse source controls the intensity, shape, and timing of the pulses, whereas the coil geometry and position determine primarily the spatial distribution of the electric field induced in the head (Peterchev et al. 2012). Around these basic components, modern TMS devices integrate various ancillary systems such as coil cooling, positioning, and field modeling, as well as electromyography and brain imaging modalities.

This chapter overviews the state of the art of TMS devices, including pulse sources with flexible control of the output waveform parameters and a wide variety of coil designs. The utility of more flexible pulse sources is supported with a review of the known effects of TMS pulse shape on the device efficiency and the brain response. The spatial stimulation characteristics of a large number of commercial and experimental coils are illustrated with electric field simulations, demonstrating a tradeoff between depth and focality. Technologies for accurate TMS targeting are discussed, including electric field models, frameless stereotaxy, and robotic coil holders. Technological aspects of ancillary coil effects such as heating, noise, vibration, and scalp stimulation are also addressed, as is the implementation of sham TMS coils. The last part of the chapter covers technical considerations for the integration of TMS and neuroimaging devices. The chapter concludes with a summary of promising ongoing and future developments in TMS technology.

Pulse Source Technology and Waveforms

TMS requires high energy pulses that present a technical challenge for the design of practical, flexible, and efficient pulse sources. Cortical TMS at the neural activation threshold requires energy of about 100 J. This is equivalent approximately to 1% of the energy stored in a typical mobile phone battery, but it has to be delivered to the stimulation coil very rapidly, in less than a tenth of a millisecond. Such high energy is required for magnetic stimulation since only a small part of the energy is transferred to the target neurons because of their poor electromagnetic coupling with the coil. Most of the energy remains in the stimulator circuit or is converted into heat. To generate the high energy pulses required for TMS, the pulse sources

deliver peak voltages in the kilovolt range (typically up to 3 kV) and peak currents in the kiloampere range (up to 10 kA) for a typical pulse width on the order of a tenth of a millisecond. The pulse sources employ an energy storage capacitor or capacitors that are charged relatively slowly from a power outlet and are discharged rapidly into the coil during the pulse delivery. Some devices store energy exceeding 1000 J to enable suprathreshold, multipulse, or pulse shaping paradigms. The power consumption of a TMS device is directly proportional to the pulse repetition rate. In some repetitive TMS (rTMS) devices the pulse repetition rate is as high as 100 Hz, corresponding to power consumption up to 10 kW at maximum pulse strength, which is equivalent to the power of eight standard electrical outlets.

In this section we discuss conventional TMS devices and recent developments of more flexible pulse shape control as well as the effect of pulse shape on the device efficiency and the brain response.

Conventional Devices

In conventional TMS devices the pulse waveform results from an oscillation of energy between the storage capacitor and the stimulation coil. Accordingly, for a given capacitor and coil, the pulse waveform has fixed shape. The two most common pulse source types are the biphasic and the monophasic stimulator.

In the biphasic stimulator, a simple oscillator is formed by connecting a charged capacitor to the stimulation coil using a high-voltage switch, typically implemented with an antiparallel combination of either a thyristor and a diode or two thyristors (see Figure 10.1(a)). As illustrated in Figure 10.1(a) the waveform shape of this device is a sine for the pulse current, which is proportional to the magnetic field, and a cosine for the corresponding coil voltage, which is proportional to the electric field. The oscillation period of the sine pulse is determined by the capacitance, coil inductance, and circuit resistance. For the conventional biphasic pulse, the oscillation is stopped after one period. Because of energy losses and associated heating in the device, the oscillation amplitude decays over time as seen in Figure 10.1(a). In a well-designed device, these losses are limited and a substantial portion of the pulse energy is recovered on the capacitor at the end of the pulse. This energy can be recycled during subsequent pulses enabling high-rate rTMS. Therefore, conventional rTMS devices almost exclusively use biphasic sinusoidal pulses, including both rTMS devices that are cleared by the US Food and Drug Administration (FDA) for the treatment of depression—the NeuroStar TMS Therapy system by Neuronetics (Malvern, PA, USA) and the Deep TMS system by Brainsway (Jerusalem, Israel).

In some devices the oscillation can be terminated only after half a period (biphasic half-wave or half-sine pulse) or after two or more periods (polyphasic or multiphasic pulse) (Figure 10.1(a)) (Wada et al. 1996; Maccabee et al. 1998; Emrich et al. 2012). After a half-sine pulse the voltage of the capacitor is inverted, so either the capacitor has to be charged back to the opposite polarity or the subsequent pulse will have inverted polarity. The pulse can also be left oscillating for multiple periods until it decays to zero, but in this case none of the pulse energy is recovered (Mc Robbie 1985).

The biphasic, polyphasic, and half-sine waveforms all involve positive and negative electric field phases with similar amplitude. It is thought that more unidirectional electric field pulses produce more selective neural recruitment (see Section Pulse Waveform effects). Therefore, a widely used class of stimulators generates monophasic magnetic pulses with a fast magnetic field rise time and a slow fall time, resulting in an asymmetric electric field pulse that is predominantly unidirectional (Figure 10.1(b)). The pulse damping is accomplished with a free-wheeling diode and resistor added across the capacitor (see Figure 10.1(b)). As a result, the oscillator performs only the first quarter cycle. After that the diode shunts a large portion of the capacitor current to the resistor and overdamps further oscillation. As a consequence, after the first quarter period, the current decays slowly back to zero (Jalinous 1991). The coil current has only a single positive phase, hence the term “monophasic.” The resulting electric field has both a positive and a

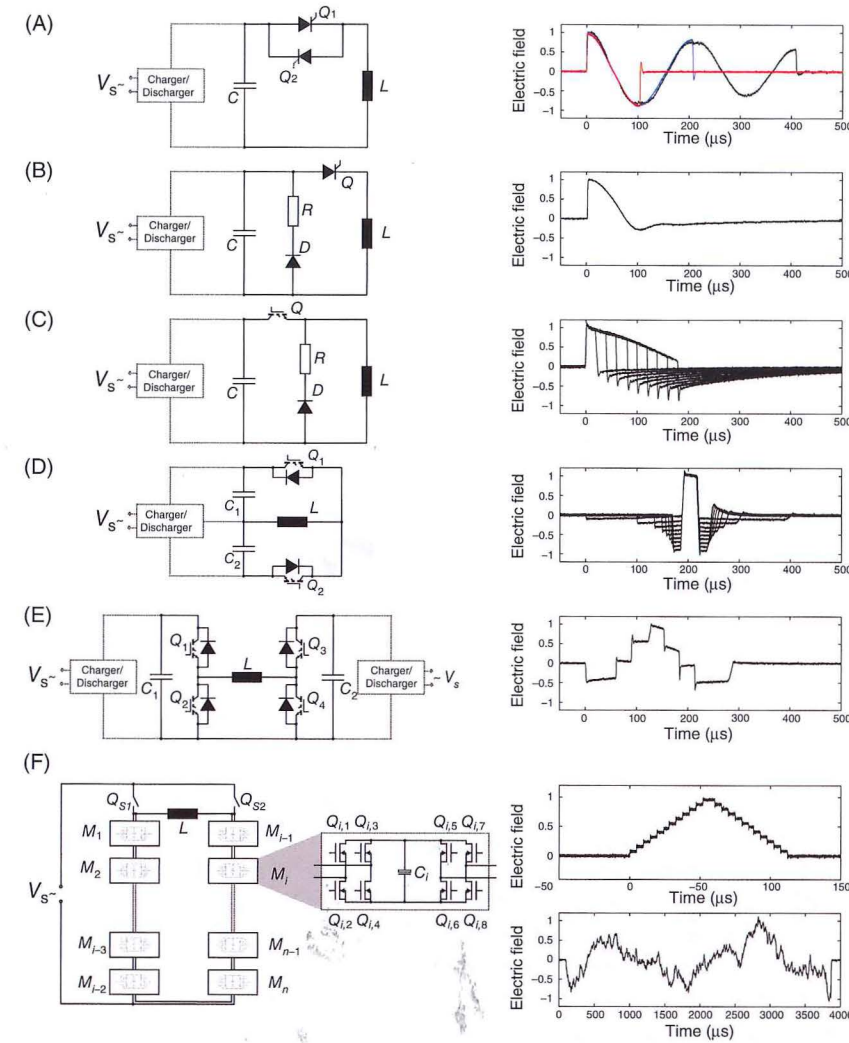


Figure 10.1 TMS pulse source types (left column) and the electric field pulses they can generate (right column). The circuit topology typically used in rTMS devices (A) generates underdamped cosine waveforms. If switch Q₂ is implemented with a diode, the sinusoidal pulse can be terminated after every full period, enabling biphasic (blue trace) and polyphasic (black trace) pulses. If switch Q₂ is implemented with a thyristor instead, the oscillation can also be terminated after half periods, which enables half-sine pulses (red trace). Conventional monophasic stimulators (B) overdampen the sinusoidal oscillation after its first quarter cycle and generate a predominantly unidirectional electric field pulse. The cTMS1 device (C) generates near rectangular pulses with adjustable pulse width. The cTMS2 (D) and cTMS3 (E) devices can control independently the amplitude and width of the rectangular pulse phases. Modular synthesizers (F) could generate pulses and pulse sequences of virtually any shape. Of these topologies all but the conventional monophasic device (B) provide efficient pulse energy recycling.

negative phase, since the electric field mean must always be zero in order to reset the coil current to zero. However, the first electric field phase is short and high amplitude, whereas the second phase is long and low amplitude. Since this conventional monophasic device uses a resistor to shape the pulse, all of the pulse energy is converted into heat and consequently lost. Therefore, while stimulation with a high pulse

repetition rate is feasible (Schmid et al. 1993), because of the high heating as well as the power required to fully recharge the capacitor after each pulse, commercially available monophasic stimulators are limited to relatively low pulse repetition rates.

Thus, commercially available TMS devices offer a limited selection of pulse shapes that is largely determined by the ease of generating sinusoidal pulses with fixed duration rather than by physiological or electrical efficiency. Most devices can generate only one type of waveform. The most flexible system currently on the market is the MagPro X100 with MagOption (MagVenture A/S, Farum, Denmark), which offers a choice among conventional monophasic, biphasic, polyphasic, and half-sine waveforms with two closely spaced pulse width settings.

Devices with Enhanced Pulse Waveform Control

To address the limitations of pulse shape control in commercial TMS devices, a number of novel devices have been demonstrated or are under development. A first-generation controllable pulse parameter device (cTMS1) that generates near rectangular electric field pulses with adjustable pulse width is depicted in Figure 10.1(c) (Peterchev et al. 2008). In contrast to the thyristor switches used in conventional TMS devices, cTMS1 uses an insulated gate bipolar transistor (IGBT) that allows the switch current to be turned off actively to achieve control of the pulse duration. The energy storage capacitor has higher capacitance value than that of conventional devices, which enables a wide pulse width range and an almost triangular current rise, corresponding to a nearly rectangular initial electric field phase illustrated in Figure 10.1(c). As in conventional monophasic stimulators, the second phase is shaped by a damping resistor that converts the pulse energy into heat.

Figure 10.1(d) depicts a second-generation cTMS device, cTMS2. It uses two energy storage capacitors, one charged to a positive voltage and one charged to a negative voltage, to enable both more flexible pulse parameter control and pulse energy recycling (Peterchev et al. 2014). The two capacitor voltages determine independently the amplitudes of the positive and negative electric field pulses. The length of time when the coil is connected to one of the capacitors is controlled by the two IGBT switches and determines the duration of the positive and negative electric field pulses. During the pulse, energy is transferred between the two capacitors, so it can be recycled in subsequent pulses, as in conventional biphasic devices. Thus, the cTMS2 device can generate efficiently monophasic, biphasic, or polyphasic pulses that induce near rectangular electric field waveforms with independently adjustable amplitude and duration of the positive and negative phases. An example of pulses with variable directionality is illustrated in Figure 10.1(d).

A variation of the cTMS2 circuit, cTMS3 shown in Figure 10.1(e), uses two positively charged capacitors and four switches (Peterchev et al. 2014). Compared to cTMS2, cTMS3 has some technical implementation advantages and allows the generation of two additional coil voltage levels. This enables more flexible shaping of the pulses, as illustrated by the staircase waveforms in Figure 10.1(e).

Finally, Figure 10.1(f) depicts a pulse synthesizer technology that may allow largely unlimited waveform flexibility (Goetz et al. 2012a). In contrast to conventional TMS devices that use a small number of high-voltage capacitors and switches, this circuit combines the output of multiple low-voltage, fast switching, independently controlled, electrically efficient modules. This approach has implementation advantages since the energy storage capacitor and switches within each module can be low-voltage. Furthermore, the independent control and fast switching speed of the multiple modules enable the synthesis of virtually any pulse waveform and sequence of pulses. The pulse energy can be recycled for all waveforms, providing low-power consumption and heating. These features of the modular pulse synthesizer could enable, for example, the efficient generation of conventional monophasic pulses (Figure 10.1(b)) at high frequencies, change of the pulse waveform during an rTMS pulse train, or complex waveforms such as the staircase

and random-noise waveforms illustrated in Figure 10.1(f). At present, a scaled-down laboratory prototype has been demonstrated (Goetz et al. 2012a). Leveraging on the modularity of the technology, it could be expanded to TMS power levels in the future.

Pulse Waveform Effects

The TMS pulse waveform affects both the technical performance of the device and the physiologic response to stimulation. From a technical perspective, some pulses are easier to generate, as discussed above, while others are more energy efficient and produce less coil heating. Physiologically, different neuron types have distinct channel expression, geometry, and anatomic surroundings that result in characteristic dynamics (Skinner and Saraga 2010; Markram et al. 2004; Maccaferri and Lacaille 2003; Chung et al. 2007). The pulse waveform interacts with the neuron dynamics and therefore may influence the neural response. While TMS, even with the most focal available coils, stimulates simultaneously a large number of neurons, specific waveforms may indeed recruit neural subpopulations with some selectivity (Di Lazzaro et al. 2012), as described in the sections below.

Energy Efficiency and Heating

Although the power consumption and heating of the TMS device do not directly affect the physiological response to stimulation, they can limit the feasibility of stimulation protocols, especially in high-power or limited-power applications, such as stimulation with small focal coils, peripheral stimulation for rehabilitation, magnetic seizure therapy, or portable stimulators (Goetz et al. 2011; Epstein 2008; Lisanby and Peterchev 2007). The energy required for a neural response and the device heating depend on the pulse waveform. Shorter pulses are more energy efficient than longer ones (Barker et al. 1991; Goetz et al. 2013; Peterchev et al. 2013). However, short pulses require higher electric field pulse amplitudes, and hence coil voltages, which limits their practicality (Goetz et al. 2013).

Rectangular electric field pulses outperform conventional sinusoidal pulses in terms of required energy and heating (Peterchev et al. 2011; Goetz et al. 2012b; Peterchev et al. 2008). In fact, optimization using neural response models suggests that the TMS waveform generating the least heating consists of a symmetric, rectangular, bidirectional electric field pulse surrounded by very low amplitude, long lead-in and tail phases (Goetz et al. 2013).

Stimulation Threshold

Biphasic pulses require stimulation amplitudes that are at least 25% lower than monophasic pulses for identical capacitors and coils (Niehaus et al. 2000; Kammer et al. 2001; Arai et al. 2005; Kammer et al. 2007). The threshold of half-sine pulses falls between that of biphasic and monophasic pulses (Sommer et al. 2006b). Increasing the number of oscillation periods of sinusoidal pulses reduces the stimulation threshold (Wada et al. 1996; Maccabee et al. 1998; Emrich et al. 2012). However, the threshold-reduction effect saturates if the total pulse length exceeds a few oscillation cycles.

The pulse polarity, which determines the direction of the induced electric field, also affects the motor threshold. On average, the lowest motor threshold results from the initial phase of the induced current flowing in the posterior-anterior direction for monophasic pulses and in the anterior-posterior direction for biphasic pulses (Brasil-Neto et al. 1992; Sommer et al. 2006b; Balslev et al. 2007). Although no phase of a pulse can be analyzed in isolation, the difference in optimal direction between monophasic and biphasic pulses can be partly explained by the direction of the strongest phase of the induced current, which is posterior-anterior in both cases (Corthout et al. 2001). The higher asymmetry of the monophasic waveform compared to the biphasic one may explain the observation that the threshold difference between the two

current directions is larger for monophasic pulses (about 20%) than for biphasic pulses (less than 10%) (Niehaus et al. 2000; Kammer et al. 2001; Arai et al. 2005). Similar to the monophasic waveform, for the half-sine pulse the induced current direction corresponding to lower threshold is posterior–anterior, but the difference between the thresholds for the two directions is less than 2% (Sommer et al. 2006b). For polyphasic pulses, the difference between the two current directions is similarly negligible (Claus et al. 1990).

For a fixed pulse shape, changes of the pulse duration also affect the neural excitation threshold. Briefer pulses require larger pulse amplitude to stimulate neurons. For the conventional range of pulse durations (tens to hundreds of microseconds), this strength–duration relationship can be well approximated by Lapicque’s leaky-integrate-and-fire model of the neural response (Lapicque 1907; Barker et al. 1991; Peterchev et al. 2013).

Input–Output Curve

The input–output (IO) curve relates the amplitude of motor-evoked potentials to the TMS pulse strength, and can therefore be used to characterize the properties of the corticospinal tract. The IO curve has a sigmoid shape with key parameters including the motor threshold, a slope, and saturation levels (Goetz et al. 2014). The IO curve slope is affected by the pulse shape and current direction (Niehaus et al. 2000; Orth and Rothwell 2004; Sommer et al. 2006b). Differences in the IO slope may be explained in part by the motor threshold shift among the various pulse shapes and current directions (Peterchev et al. 2013). Furthermore, longer pulse widths result in steeper IO curve slope (Rothkegel et al. 2010; Peterchev et al. 2013). The IO slope dependence on pulse width can be explained by the leaky-integrator characteristic of neural membranes, which also explains the strength–duration curve of the stimulation threshold (Peterchev et al. 2013).

Motor Response Latency

The latency of cortically evoked muscular responses is shortest for biphasic stimuli, longest for monophasic pulses, and intermediate for half-sine pulses (Sommer et al. 2006b). The differences in the latency of the compound muscular response, which is a summation of all nervous motor signals arriving in the specific muscle, are usually ascribed to a different pattern of early, direct (D) and later, indirect (I) waves in the corresponding corticospinal axons. The characteristic spiking patterns of D- and I-waves are most likely an indicator of the activation of different neuron populations that feed the same output path (Edgley et al. 1997; Day et al. 1989). For monophasic stimuli with initially posterior–anterior induced current direction, the first I-wave emerges at low stimulation amplitudes, whereas later I-waves and a D-wave appear at higher amplitudes (Di Lazzaro et al. 2012). If the current direction is reversed, the timing of the I-waves changes slightly, and a D-wave may emerge at lower amplitudes. In contrast, the corticospinal waves induced by biphasic stimuli have a less pronounced pattern and resemble a combination of the effects of monophasic pulses of both current directions (Di Lazzaro et al. 2012). This observation suggests that compared to biphasic pulses the more unidirectional electric field of monophasic pulses produces more selective stimulation of different neuron populations in the cortex.

Contralateral Silent Period

The contralateral silent period, a measure of intracortical excitability, is sensitive to the pulse waveform as well. Monophasic pulses with posterior–anterior induced field direction may cause a shorter contralateral silent period than both monophasic pulses with anterior–posterior field direction and biphasic pulses, although the data are not conclusive (Orth and Rothwell 2004; Sommer et al. 2006b). Moreover, longer pulses reduce the variability of contralateral silent period measurements (Rothkegel et al. 2010).

Repetitive TMS Effects

Potentially because of the differential neural recruitment with different pulse waveforms, the waveform affects the neuromodulation induced with rTMS. For the typically inhibitory 1 Hz protocol, monophasic pulses are more effective than biphasic pulses in influencing the motor cortex (Taylor and Loo 2007; Sommer et al. 2002), the premotor cortex (Hosono et al. 2008), and the visual cortex (Antal et al. 2002). Similar observations were also made for higher repetition rates applied to the motor cortex (Arai et al. 2005; Tings et al. 2005; Arai et al. 2007). For both low- and high-rate rTMS in the motor cortex, the current direction with the higher threshold may induce stronger effects than the lower threshold current direction (Sommer et al. 2013).

Coils

The locus of neural activation by TMS depends on the induced electric field distribution that, in turn, depends on the geometry and placement of the stimulating coil. In this section we discuss various coil configurations and their electric field characteristics as well as technical advances in coil field modeling, positioning systems, efficiency and cooling, noise and scalp stimulation, and sham. The clinical effects of different TMS coils are discussed in Chapter 12.

Types of Coils

A wide variety of coils have been evaluated or proposed for TMS. A collection of 61 coil models is illustrated in Figure 10.2 with corresponding electric field simulations in a spherical head model depicted in Figure 10.3 (in this section we refer to the coils by their number assigned in Figure 10.2). Several of these coils have found extensive use and are available commercially. The subsequent sections address the more notable coils; further discussion can be found in Deng et al. 2013.

To allow a systematic comparison of the large-scale electric field features among various TMS coils designs, the field depth and focality can be quantified with two metrics (Deng et al. 2013): *Depth* is defined as the radial distance from the cortical surface to the deepest point where the electric field strength is half of its maximum value on the surface. *Spread* quantifies focality and is defined as the volume of the brain region that is exposed to an electric field as strong as or stronger than half of the maximum electric field, divided by *depth*. To illustrate the relationship between coil focality and depth of stimulation, Figure 10.4 plots *spread* as a function of *depth* for the 61 TMS coil configurations from Figure 10.2.

Conventional Circular and Figure-8 Coils

Commercial TMS devices are typically accessorized with two types of coils: circular and figure-8. Circular coils induce a nonfocal ring-shaped electric field maximum potentially stimulating a swath of brain regions under the coil perimeter. For example, a typical circular configuration is the Magstim (Whitland, Carmarthenshire, UK) 90 mm round coil (#9). Because of their nonfocality, conventional circular coils are rarely used for TMS nowadays.

The most commonly used coil type is the figure-8 configuration. The figure-8 configuration consists of a pair of adjacent circular loops with current flow in opposite directions, producing a relatively focal electric field maximum under the center of the coil where the two loops meet. The Magstim 70 mm double coil (#38) is a typical example. Compared to the circular coils, the figure-8 coils have improved focality (see Figures 10.3 and 10.4). Their focal field makes figure-8 coils suitable for functional mapping of the cortex and for targeted neuromodulation. For example, the Navigated Brain Stimulation System by Nexstim

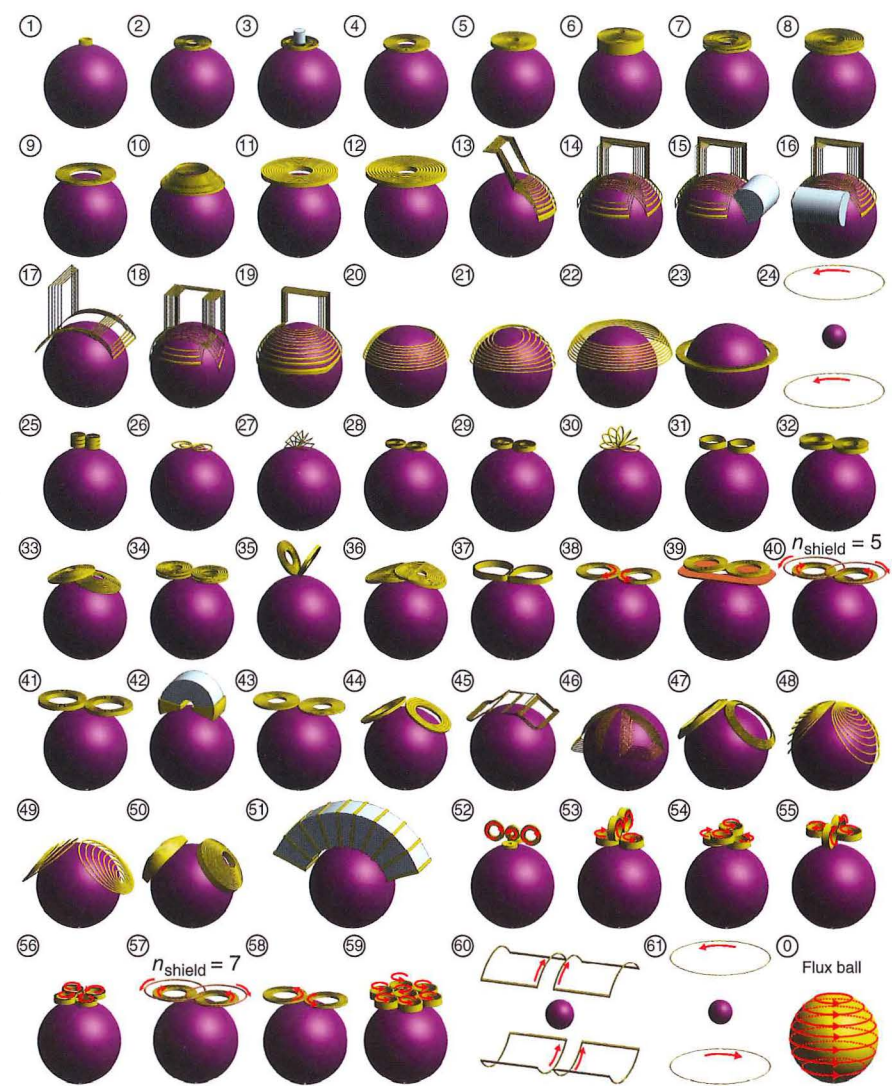


Figure 10.2 Simulation models of 61 TMS coil configurations. Included are coils developed by Brainsway (13–19, 45–46), Magstim (2, 4, 7–10, 28, 38, 47, 58), Cadwell (31, 37), MagVenture (6, 34, 36, 44, 50), Neuronetics (42), Neurosoft (5, 11, 12, 29, 33, 41), and Nexstim (32, 43). Modified from (Deng et al. 2013) that contains more extensive descriptions of the coils. Acknowledgment to Drs. A. Zangen (Ben-Gurion University of the Negev/Brainsway) and R. J. Ilmoniemi (Aalto University/Nexstim) for providing parameters for the H coils and Nexstim coils, respectively.

(Helsinki, Finland) uses figure-8 coils (#29 and #32) and is approved by the FDA for cortical mapping prior to neurosurgery. Further, the Neuronetics NeuroStar TMS system incorporates a figure-8 type coil with a ferromagnetic core (#42).

Strategies for Increasing Stimulation Focality

Generally, focality can be enhanced by reducing the diameter of the coil windings; smaller coils are more focal because the magnetic flux is more confined. Small coils, however, have fast attenuation of the electric

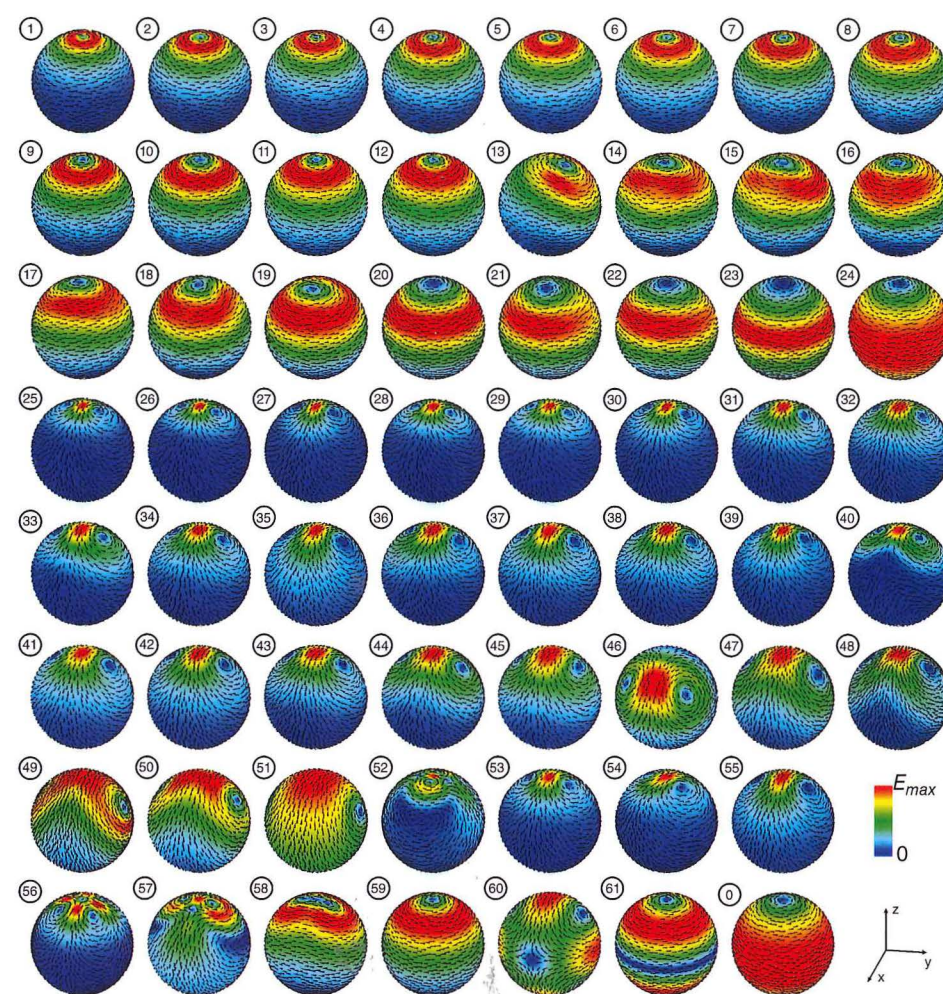


Figure 10.3 Induced electric field distributions of the TMS coils from Figure 10.2. The electric field is shown on the brain surface of a spherical head model. For each coil, the field magnitude is plotted with a color map normalized to the field maximum in the brain. The arrows indicate the electric field direction. Modified from Deng et al. 2013, 2014.

field with distance and have limited feasibility because of the high forces and heating occurring within a small volume. Various attempts have been made to increase focality of TMS coils while circumventing these challenges. To focalize the stimulation site, circular coils have been modified with an angulated extension or with variation of the winding density or concavity (Cohen and Cuffin 1991; Cadwell 1991). However, none of these approaches significantly enhances the circular coil's focality. Attempts to improve the stimulation focality of figure-8 type coils include:

- (1) The “cloverleaf” coil design, which consists of four sets of nearly circular windings (#56) and is more efficient in stimulating long fibers compared to the figure-8 coil (Roth et al. 1990);
- (2) The “Slinky” coil design, which consists of multiple circular or rectangular loops joined together at one edge and fanned out to form a half toroid (#27 and #30) (Ren et al. 1995);

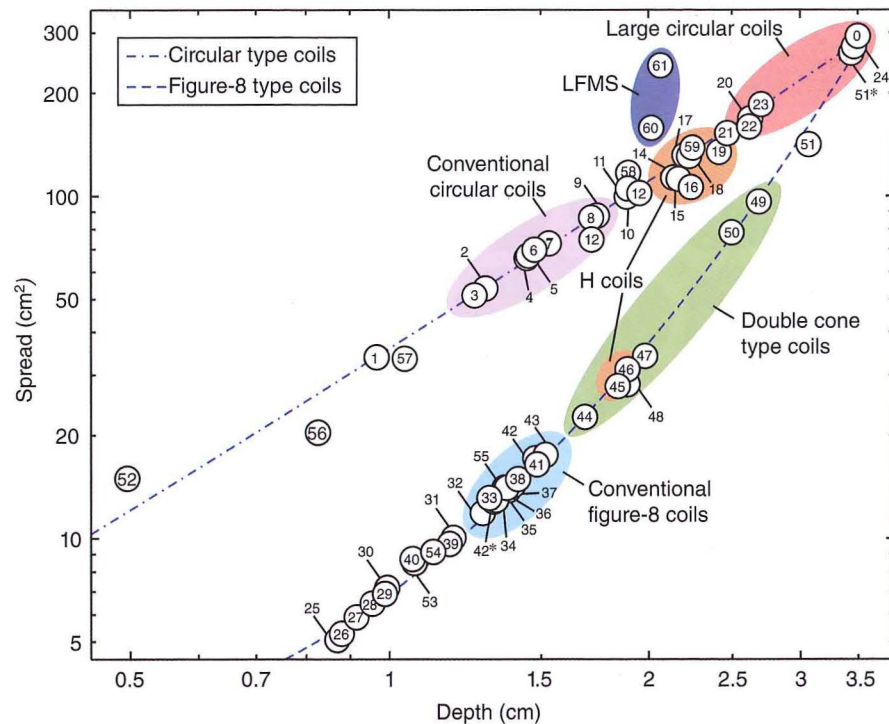


Figure 10.4 Electric field spread, quantifying focality, versus electric field depth for the TMS coils in Figure 10.2. The plot illustrates the depth–focality tradeoff for TMS coils. Modified from Deng et al. 2013, 2014.

- (3) The eccentric figure-8 coil, which has higher density of winding turns toward the center of the coil than in the periphery (#26) (Knäulein and Weyh 1996);
- (4) The 3-D differential coil (#52), consisting of a small figure-8 coil with a third loop positioned perpendicular to the center of the figure-8 coil and flanked by two additional loops to restrict the area of stimulation, which provides more focal stimulation compared to the figure-8 and slinky coils (Hsu and Durand 2001);
- (5) Control of the coil focality and electrical properties with the use of litz wire (Schmid et al. 1993) and active or passive shielding (Hernandez-Garcia et al. 2010, Kim et al. 2006).

These coils generally have better focality compared to the regular figure-8 coils of the same outer dimensions. They may have advantages over smaller coils, which are also more focal, since small windings are harder to manufacture and cool. Shielding can provide more flexibility since a range of field characteristics can be obtained by adjusting the geometry of the conductive shielding plate or the current of the active shielding coil without the need to modify the stimulation coil itself. Coil shielding, however, increases losses because of the added conductive paths and reduces the coil inductance, which may in turn affect the stimulator operation.

Strategies for Increasing Stimulation Depth

In parallel with the attempts to optimize TMS focality, there have been efforts to increase the depth of stimulation in order to stimulate directly deep brain structures. Generally, coils with larger dimensions

induce a more deeply penetrating and less focal electric field compared to smaller coils, as illustrated in Figure 10.4. A family of designs called “Hesed” (H) coils manufactured by Brainsway are used for deeper stimulation compared to conventional TMS coils (Roth and Zangen 2006). More than twenty different types of H coils have been designed and used in several dozens of clinical trials (Roth et al. 2013; Bersani et al. 2013). An rTMS system using the H1 coil (#14) has FDA clearance for the treatment of depression. The H coils typically have complex winding patterns and larger dimensions compared to conventional TMS coils, and consequently have slower electric field attenuation with depth, at the price of reduced focality (see Figures 10.3 and 10.4). H coils #13–#19 induce an approximately circular electric field pattern with greater *depth* and *spread* than conventional circular coils. Other H coils (#45 and #46) have an electric field distribution similar to those of double cone type coils, although the standard Magstim double cone coil (#47) and the MagPro twin coil (#50) induce a deeper field.

Other proposed designs that induce even deeper electric fields than H coils, at the price of further focality reduction, include the stretched C-shaped ferromagnetic core coil (#51) (Davey and Riehl 2006, Deng et al. 2014), circular crown coil (#20–#22) (Deng et al. 2014), and large halo coil (#23) (Crowther et al. 2011).

Low-field Magnetic Stimulation

There is accumulating evidence that the subthreshold electric field induced in the brain by the gradient coils in magnetic resonance imaging (MRI) scanners affects brain activity. This low-field magnetic stimulation (LFMS) has been reported to influence glucose metabolism in the brain (Volkow et al. 2010) and to exert antidepressant effects in humans (Vaziri-Bozorg et al. 2012; Rohan et al. 2004) and in animals (Carlezon et al. 2005; Rokni-Yazdi et al. 2007; Aksoz et al. 2008). The MRI gradient coils used in LFMS studies (#60 and #61) induce more diffuse electric field compared to TMS coils with comparable depth of field penetration, as illustrated in Figures 10.3 and 10.4.

Multichannel Arrays

Finally, another line of work on improving magnetic stimulation targeting concerns the use of independently controlled multichannel coil arrays (Ruohonen and Ilmoniemi 1998). The major advantage of such a system is the flexibility of controlling the spatial electric field distribution and the ability to stimulate several brain areas simultaneously or in rapid succession. Multichannel arrays do not circumvent, however, the fundamental depth–focality tradeoff of electric field targeting. Moreover, such systems face implementation challenges such as cross talk between the channels that may distort the applied pulse waveforms and potentially damage the semiconductor switches; high losses, heating, and forces in the relatively small coil elements; as well as uneven focusing ability across the brain surface because of coarse electric field quantization due to the infeasibility of very small coil elements.

Summary: Stimulation Depth–Focality Tradeoff

As demonstrated in Figure 10.4, among coil designs there is a tradeoff between electric field depth of penetration and focality. Specifically, deeper electric field penetration is achieved at the price of reduced focality. Coil elements with larger dimensions generate an electric field that penetrates deeper but is less focal than that of smaller coil elements. Therefore, larger coils may be associated with an increased risk of seizures and other side effects.

Figure 10.4 further suggests that in most cases the electric field generated by TMS coils can be described as circular or figure-8 type. Figure-8 type coils are fundamentally more focal than circular type coils. For large coil sizes, the difference in the depth–focality ratio between circular and figure-8 coils diminishes. It is noteworthy that none of the coil designs overcomes the depth–focality tradeoff set by the figure-8 type coils. Hence, no TMS coil can achieve deep and focal stimulation simultaneously.

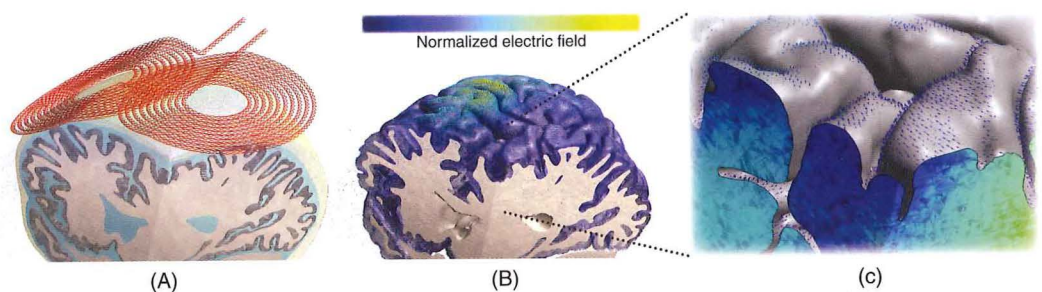


Figure 10.5 Electric field simulation with realistic head and coil models. The head model is based on a structural MRI scan and has accurate rendering of the brain gyri. The coil model represents accurately the (A) winding wire shape, (B) dimensions, and (C) structure (litz wire, reduced to a four-strand conductor for better visibility). The illustration was generated with the t.e TMS brain field simulation toolkit in combination with modules from SimNIBS, GetFEM++, Gmsh, and Blender. Courtesy of M. S. Singer and S. M. Goetz.

Electric Field and Neural Response Models

In addition to the coil type and position, the head anatomy also affects the electric field induced in the brain. Since the induced electric field mediates the effect of TMS, accurate electric field models can contribute to coil design for optimal targeting of particular brain structures, to appropriate selection of the TMS dose, and to better understand TMS mechanisms. While spherical models remain useful for TMS coil design and evaluation, for some parametric studies, as well as for a standardized replicable reference, they lack accurate geometric representation of the head tissues. State-of-the-art realistic head models have been developed to include the individual gyral geometry of the brain based on structural MRI data as well as white matter anisotropic conductivity based on diffusion tensor MRI (see, for example, Figure 10.5) (Windhoff et al. 2013; Opitz et al. 2011; De Geeter et al. 2012; Toschi et al. 2012; Opitz et al. 2013). The increased precision of the electric field distribution estimate in realistic head models provides important insights. For example, spherical models result in the absence of radial current flow normal to the tissue interfaces in the brain, whereas currents normal to the tissue boundaries do occur in realistic models. Further, because of tissue heterogeneity and individual differences in cortical folding, the site of maximum induced electric field is not always directly underneath the center of the coil (Bijsterbosch et al. 2012; Thielscher et al. 2011). Therefore, electric field simulation in realistic head models could inform the optimization of coil designs to optimally target specific brain regions, as has been done for transcranial electric stimulation (Dmochowski et al. 2011).

At present most TMS modeling studies treat the electric field distribution as the end point. However, temporal aspects of stimulation have to be considered in a more complete analysis of the extent of neural activation by TMS. Structurally detailed models capable of accurately predicting cortical activation for a given induced electric field distribution could provide a critical resource for understanding the functional consequences of TMS. While such efforts have been limited so far, future studies should incorporate accurate models of the neural response to the electric field (Agudelo-Toro and Neef 2013). Furthermore, simulating the neural population response to single and multiple pulses would require linking the individual neurons in a network model (Esser et al. 2005).

Coil Positioning

Frameless Stereotactic Neuronavigation

Accurate, stable, and reproducible coil placement is critical for targeted TMS. In research applications of TMS, frameless stereotactic navigation has become a common support tool over the past decade. Originally

derived from applications in surgery (Kato et al. 1991; Roberts et al. 1986), present frameless stereotactic systems typically use optical tracking of reflective or active light-emitting markers with infrared stereo cameras (Tebo et al. 1996). The markers are mounted on the coil and the subject's head and localized in space by rapid-rate triangulation by the camera and the associated software. The readout of the orientation of an object requires at least three markers attached to it. When the markers are initially mounted on the object, a registration procedure is required to calibrate the position of the markers relative to the object.

Navigated TMS enables detecting and maintaining the coil position. When coregistered with anatomical or functional brain scans, frameless stereotaxy enables positioning of the coil over specific brain targets. A navigated TMS system by Nexstim is cleared by the FDA for use in presurgical mapping (Bowsher and Eydelman 2012).

An important limitation of neuronavigation systems is their ostensible accuracy. Although the precision with which the camera and software track the markers can be less than a millimeter (Khadem et al. 2000), there are several error sources that can reduce the accuracy. Systematic absolute errors can be introduced by the 3D registration of the coil and the subject. In some systems, the accuracy of the coil registration may be affected by the tilting of a registration block or pointer relative to the coil. Furthermore, movements of the trackers relative to the subject or the coil they are attached to may lead to increasing error during a TMS session. It is advisable to avoid markers on long lever arms that can swing, narrow flexible headbands, or markers on muscles such as on the forehead. Even with appropriate care in handling, localization errors of at least 5 mm should be assumed (Ruohonen and Karhu 2010).

Several available neuronavigation systems incorporate an estimate of the induced electrical field in the cortex, although the electric field simulation is simplified to allow real-time computation. With further growth of computational power, the fusion of neuronavigation software and electric field simulation based on individual realistic head and coil models will likely be an important trend in the future. In addition to a more accurate targeting of certain functional or anatomic structures, neuronavigation with a realistic electric field model could enable appropriate selection of the pulse amplitude, especially for targets outside the primary motor cortex.

Another upcoming development may involve tracker-free navigation that has been developed in the context of computer vision (Baltrušaitis et al. 2012; Yang et al. 2005; Murphy-Chutorian and Trivedi 2009). Such systems track the location of the head based on structural as well as textural features. Since there are no tracker registration and movement issues, and since the software can incorporate a high number of reference points on the tracked object for error compensation, the accuracy and long-term stability may potentially be better than those of currently available TMS navigation setups.

Robotic Coil Holders

Whereas neuronavigation aids the user in placing the coil manually at the target, maintaining the coil targeted during a TMS session is challenging since it can cause fatigue in a human operator or, in the case of a fixed mechanical holder, subject movements can cause drift of the coil position relative to the head. To address these issues, robotic coil holder systems have been developed (Kantelhardt et al. 2010; Lancaster et al. 2004; Zorn et al. 2012). These devices incorporate a neuronavigation system that provides information about the head location for positioning the coil and correcting detected deviations. The coil position can be calculated either from the robot's joint positions or from optical markers. Furthermore, robotic systems can, in principle, quickly change the coil position between different targets in procedures such as cortical mapping.

Practical implementation of robotic coil positioning systems is still under development and has limitations. First, coil positioning systems are currently speed-limited for safety reasons because robots can generate strong forces. Accordingly, current systems cannot compensate free movement, and the subject is still supposed to sit relatively still. The speed limits also adversely affect the practicality of rapid target

changes. Second, the robot control relies on data from an optical navigation system and thus inherits the potential error sources discussed in the previous section. Third, robotic systems that rely solely on position information and do not use pressure feedback to control the contact between the subject's head and the coil may be uncomfortable to the subject and affect position accuracy because the coil is unable to follow small head movements and either presses too strongly against the head or drifts away if the subject leans against it (Zorn et al. 2012).

Coil Efficiency and Cooling

A substantial portion of the energy delivered to the coil is lost in the electrical resistance of the coil windings and cables, resulting in the heating of the coil. In rTMS the increase in coil temperature can be significant, limiting the allowable train parameters including frequency, amplitude, and duration. Coil heating can be curbed by increasing the coil and pulse electrical efficiency, improving the passive thermal properties of the coil, and/or adding active coil cooling with a circulating fluid or air (Weyh et al. 2005). An increase of electrical efficiency by more than three-fold can be achieved by incorporating a ferromagnetic core in the coil, which reduces the amount of stored magnetic energy (Lorenzen and Weyh 1992; Davey and Epstein 2000; Epstein and Davey 2002; Peterchev et al. 2011). For example, the figure-8 coil supplied with the Neuronetics NeuroStar TMS system (#42 in Figure 10.2) contains a ferromagnetic core that provides high efficiency, obviating the need for active coil cooling. The use of litz wire for the coil winding can further reduce the losses caused by high-frequency effects (Weyh et al. 2005). Liquid cooling approaches use deionized water, mineral oils, or synthetic polymers, and are generally more effective but also more expensive than air cooling.

Noise, Vibration, and Scalp Stimulation

The most common complaint reported in TMS trials is the local muscle activation and pain under the coil, which can lead to mild headache in some subjects (Rossi et al. 2009). The intensity of pain depends on individual sensitivity, site of stimulation, as well as coil and stimulus parameters. Attempts to reduce the scalp discomfort with device modifications have had limited success. Foam padding between the coil and the scalp can isolate the coil's mechanical vibration, and has been shown to reduce pain intensity by ~7% at motor threshold (Borckardt et al. 2006). A small secondary coil can be integrated on the surface of the main TMS coil to reduce the superficial electric field, but the scalp field reduction is only 9–13% (Davey and Riehl 2006), and the thin insulation of the secondary coil may break down and cause scalp burn (Rossi et al. 2009). Increasing the TMS coil size can substantially reduce the scalp electric field strength (Davey and Riehl 2006; Deng et al. 2014), but also reduces the focality of the coil (Deng et al. 2013). Finally, altering the pulse shape characteristics could be explored as a means of modulating the sensory threshold of the scalp nerves (Geddes 1987), but no experimental data have been published on this approach.

The vibration of the conductors carrying the pulsed current also results in a clicking noise that could be unpleasant to the subject, produce unintended neuromodulation effects in the brain, and cause hearing loss if hearing protection is not properly applied. While some commercial TMS devices are quieter than others because of the mechanical design of the coil, cable, and pulse source, at present there are no effective solutions that dramatically reduce the noise.

Sham

In order to quantify the difference between active and placebo response, psychophysiological and clinical studies with TMS often require a valid sham stimulation condition. The ideal sham condition should have no physiological effect on the cortex while emulating all of the ancillary aspects of TMS,

including the device appearance as well as the sound, vibration, and cutaneous stimulation produced by the coil.

A commonly used sham condition involves tilting the coil at a 45° or 90° angle from its "active" placement tangential to the head. Studies with intracerebral voltage measurements in a nonhuman primate (Lisanby et al. 2001), motor threshold evaluation (Loo et al. 2000) and PET imaging (Kimbrell et al. 2002) in healthy human subjects, and electric field simulation in a human head model (Toschi et al. 2009) suggest that the coil-tilt conditions result in substantial active stimulation and are therefore inadequate as a true sham condition.

Another sham TMS strategy employs electronically switchable coils that have the ability to deliver active and sham TMS in which the coil current in one of the windings can be reversed (Ruohonen et al. 2000). In sham mode, the coil was unable to induce motor-evoked potentials even at maximum stimulator output (Hoeft et al. 2008), but induced similar auditory-evoked potentials as active TMS (Ruohonen et al. 2000). The main limitation of this approach is that the peak electric field shifts to the coil periphery in sham mode, which can stimulate a broad brain volume surrounding the target and can affect scalp sensation (Deng and Peterchev 2011). Some of these limitations are addressed in a proposed electronically switchable quadrupole coil design with improved sham-mode electric field characteristics compared to the reverse-current figure-8 coil, including lower field penetration depth, preserved focality, and better replication of the active-mode scalp electric field pattern (Deng and Peterchev 2011). Nevertheless, complete suppression of the brain electric field in sham-mode TMS while replicating identical active-mode scalp sensation remains challenging.

Other sham TMS approaches include the use of conductive shielding plates and/or spacers to reduce the field strength (Davey 2002; Rossi et al. 2007; Sommer et al. 2006a) and the use of a smaller coil housed in a conventional coil case, which does not emit a strong field and can provide some level of discharge noise (Hovey and Jalinous 2006). However, these sham strategies abolish not only direct brain stimulation but also the induced scalp stimulation. Synchronous electric stimulation can be used to mimic scalp sensation (Mennemeier et al. 2009; Rossi et al. 2007). This strategy typically requires a dedicated passive coil and in some cases an additional active coil placed near the subject to reproduce the coil discharge sound (Okabe et al. 2003b). However, it has been reported that non-TMS-naïve subjects were able to discriminate between the electrical and magnetic stimuli, as the former were perceived as sharper (Mennemeier et al. 2009; Arana et al. 2008). Further, there could potentially be brain stimulation effects even from the weak electrical stimulation.

Technical Aspects of Concurrent TMS and Neuroimaging

To probe changes in brain activity resulting from TMS, it can be combined with concurrent neuroimaging techniques including electroencephalography (EEG), functional MRI (fMRI), positron emission tomography (PET), single photon emission computed tomography (SPECT), and functional near-infrared spectroscopy (NIRS). TMS-compatible EEG and NIRS systems as well as MRI-compatible TMS systems are available commercially. Concurrent TMS and magnetoencephalography (MEG) is not feasible with present techniques since MEG involves detection of magnetic fields that are 15 orders of magnitude weaker than the TMS pulses (Siebner et al. 2009). This section summarizes technical considerations for the integration of TMS and neuroimaging devices.

Electroencephalography

The ongoing brain electrical activity during TMS can be imaged with simultaneous EEG (Ilmoniemi et al. 1997; Ilmoniemi and Kićić 2010). EEG detects brain-generated electrical potentials in the 10–100 µV range

on the scalp and has a temporal resolution on the order of milliseconds, which makes it suitable for studying the immediate aftereffects following a TMS pulse. The spatial resolution of EEG is on the same order as the interelectrode distance, which in high-density (≥ 64 – 256 channels) applications can be as small as a few millimeters. However, this resolution is relevant only for superficial brain areas, since EEG cannot accurately map activity in deeper structures.

For TMS compatibility, the recording electrodes should be slotted and/or made out of low-conductivity material (e.g., conductive plastic coated with silver epoxy) to reduce ohmic heating from induced eddy currents in the electrodes (Roth et al. 1992). The recording electrodes should be as thin as possible in order to minimize the added distance between the coil and the scalp (Siebner et al. 2009). Finally, in order to minimize artifact caused by thermal voltage noise, and electrode movements and polarization, the electrode-to-scalp interface should be prepared with abrasive gel and conductive paste to maintain the electrode impedance below $5\text{ k}\Omega$. Active electrodes with integrated preamplifiers can reduce the noise from high electrode impedances up to the $100\text{ k}\Omega$ range.

The major problem when applying TMS during EEG recording is the large inductive and electrostatic TMS artifact that is superimposed on the EEG signal. The strong magnetic pulse emitted by the TMS coil induces voltages and currents in the loops formed by the electrode leads, amplifier circuits, and the head. Further, the high voltage applied to the coil conductor can get capacitively coupled to the EEG electrodes and leads adding an electrostatic artifact. The total artifact voltage can be several orders of magnitude larger than the intrinsic neural signal and may saturate the amplifier for seconds or longer. Amplifier saturation can be alleviated with one of the following methods: (i) using a sample-and-hold circuit that latches the signal immediately prior to the TMS pulse, pins the amplifier output during the pulse, and recovers after the pulse with a delay within tenths of a millisecond (Virtanen et al. 1999); (ii) using an amplifier with a low slew rate ($\sim 0.07\text{ V }\mu\text{s}^{-1}$) in order to limit the circuit's response to the fast-changing TMS pulse (Ives et al. 2006); and (iii) using a dc-coupled amplifier with a wide dynamic range that is sufficient to prevent saturation (Bonato et al. 2006). Artifact can be further reduced by using braided wire leads and coaxial cables to minimize the induction loop area and provide electrostatic shielding. Residual TMS-induced voltages as well as muscle artifact could be subtracted during postprocessing of the EEG signal using, for example, independent component analysis or Kalman filter based methods (Korhonen et al. 2011, Litvak et al. 2007, Morbidi et al. 2007).

Functional Magnetic Resonance Imaging

To generate a 3-D map of the hemodynamic response associated with brain activity during and immediately after TMS administration, TMS can be applied concurrently with fMRI (Bohning et al. 1998, Bestmann et al. 2008). fMRI has a spatial resolution of millimeters and a temporal resolution of seconds.

The principal technical challenges in concurrent TMS-fMRI include the MR artifact generated by the TMS coil and the increased forces on the coil because of the strong static magnetic field in the scanner. Ferromagnetic materials in the TMS coil distort the scanner magnetic field and should therefore be removed. Magnetic field distortion because of the TMS coil magnetic susceptibility can be further corrected with passive shimming on the TMS coil surface (Bungert et al. 2012). The TMS device electronic controls, capacitor charging and discharging, and line noise can result in radiofrequency (RF) noise propagated either through air or through the TMS coil. To mitigate RF interference from the TMS device, the pulse source and the stimulator control circuits are placed either outside of the scanner room or in an RF-shielded enclosure in the scanner room. This generally requires an increased length of the cable connecting the pulse source and the TMS coil. To compensate for the resulting increased resistive and inductive losses, larger diameter cable or multiple parallel cables may have to be used. Furthermore, to prevent RF noise propagation from the pulse

source to the scanner room, a high-voltage, high-current RF filter or a ferrite RF choke has to be mounted on the coil cable where it crosses the RF shield (e.g. scanner room penetration panel). Preferably, the TMS device capacitor recharging after a pulse should be delayed until after the MRI acquisition sequence is complete. In addition, it is necessary to deploy a shunting circuit in parallel with the TMS coil to reduce magnetic-field distortion artifact caused by weak currents (up to 1 mA) flowing continuously through the coil because of leakage in the pulse source high-voltage switch (Weiskopf et al. 2009). The transient artifact resulting from the TMS pulse is very strong but subsides typically within 100 ms (Bestmann et al. 2003; Bohning et al. 2003a). Its effect on the MR images can be diminished by properly interleaving the TMS pulses with the imaging sequence (Shastri et al. 1999; Bestmann et al. 2003). To curb the TMS pulse artifact and to protect the MRI head coil electronics from the eddy currents induced by the TMS pulse, it is advisable to keep the TMS coil away from the surface of the head coil.

Because of the strong static magnetic field in the MRI scanner, the electromagnetic forces in the TMS coil are increased up to 2.5-fold (Crowther et al. 2012). This requires the use of special, mechanically reinforced TMS coils. Only coil configurations that do not produce net force or torque can be used in the scanner. This rules out, for example, circular and figure-8 type coils with angled loops. The conventional symmetric figure-8 coil configuration with loop currents flowing in the opposite direction is acceptable because the forces and torques in the two loops cancel each other. Further, only zero-mean biphasic magnetic pulses should be delivered in order to temporally average out the internal strain in the TMS coil. Nevertheless, the shape of the electric field pulse can be varied by controlling the rise and fall times as well as the duration of the phases of the zero-mean magnetic pulse, for example with the pulse source circuits shown in Figure 10.1(d–f). Because of increased forces in the coil as well as reverberation in the scanner bore, the coil click sound is stronger in the scanner (Bohning et al. 1998). Consequently, hearing protection and noise masking are even more important for TMS in the scanner than for stand-alone TMS. To ensure accurate targeting and to reduce vibration, the TMS coil has to be fixed with an MRI-compatible coil holder (Bohning et al. 2003b; Moisa et al. 2009). To accommodate the TMS coil holder, the MRI head coil should be large enough and have an open design.

Positron Emission Tomography and Single Photon Emission Computed Tomography

Traditionally, PET is used for blood flow and glucose-metabolic-rate imaging of brain activity. In many applications PET is being phased out by fMRI, since the spatial resolution (~ 5 – 15 mm) and the scanning time (minute range, dependent on the tracer activity) are worse (Bettinardi et al. 2011). In the future, PET may play a more important role because of its ability to image specific molecules with appropriate labeling, for example neurotransmitters, such as dopamine or serotonin, and their receptors (Farde et al. 1986; Strafella et al. 2003; Suehiro et al. 1993; Sibon et al. 2007; Drevets et al. 1999).

Since PET does not provide any structural data, almost all modern PET devices incorporate another imaging modality, which reduces errors associated with coregistration of separate scans (Wassermann et al. 1996). The structural imaging modality is, in most cases, computed tomography (CT). More recently, the integration of PET with MRI has advanced after solving compatibility issues between the photodetectors and magnetic fields (Catana et al. 2012; Judenhofer et al. 2008). Accordingly, this development enables simultaneous combinations of structural, tensor, and functional MRI with the biochemical imaging capabilities of PET.

The requirements for integrating TMS in a PET scanner are fewer than for concurrent TMS-fMRI since the magnetic fields of TMS pulses do not interact with the photon emission (Siebner et al. 2009). Therefore, in contrast to TMS-fMRI, the pulse timing does not have to be synchronized to the scanning procedure, providing more flexibility for online imaging during various rTMS paradigms (Takano et al. 2004; Siebner

et al. 2001). To prevent electric artifacts and potential damage in the PET scanner photomultipliers by the TMS pulses, thin permalloy, or metal shielding over the photomultipliers may be advantageous (Siebner et al. 1999).

In comparison with PET, SPECT has similar or lower spatial resolution (~1 cm) and notably longer scan duration between 10 minutes and half an hour (Hutton 2010). Because of the long scan time, SPECT has been used exclusively with offline TMS (Nahas et al. 2001; Okabe et al. 2003a; Hosono et al. 2008).

Functional Near-Infrared Spectroscopy

The hemodynamic response to TMS can be imaged with concurrent functional NIRS, sometimes referred to as fNIR. Neurovascular coupling allows neural activity in the brain to be inferred from the hemodynamic signal, similarly to fMRI. TMS–NIRS has several advantages including the absence of electromagnetic interference from the TMS pulse to the optical signal, better temporal resolution than PET and fMRI, small and portable imaging equipment, and excellent safety profile (Nasi et al. 2011; Siebner et al. 2009). The principal disadvantages of NIRS are the limited spatial resolution (~1 cm) and imaging depth (superficial cortex) (Wolf et al. 2007; Siebner et al. 2009).

In addition to these features, several considerations are relevant for the successful integration of TMS and NIRS. The thickness of the NIRS optical probes on the head should be minimized to prevent the reduction of the TMS stimulation strength because of increased coil-to-cortex distance. Furthermore, the mechanical contact with the TMS coil and the coil vibration can disturb the position of the optical probes causing an artifact. Finally, TMS produces hemodynamic changes not only by influencing neural activity but also through other mechanisms including potentially local effects on the vasculature or global arousal effects (Nasi et al. 2011). Therefore, TMS–NIRS studies have to carefully control for physiological artifact that is not related to the direct effect of TMS on cerebral activity.

Conclusion and Future Directions

Advances in the capabilities of TMS technology could enable novel, more effective paradigms in research and clinical applications. Building on the recent development of pulse sources with flexible pulse parameter control, future TMS devices could allow enhanced probing and neuromodulation by leveraging the dependence of the neural response on the stimulus waveform. For example, novel pulse source circuits could generate rTMS pulse shapes that yield stronger and more selective neuromodulation. Optimized pulse shapes can also reduce the device power consumption and coil heating.

While TMS is unable to produce direct focal deep stimulation, electric field simulations in realistic head models could aid the optimization of coil designs to target specific brain regions. The implementation of real-time, individual electric field simulation and the integration of neural response estimation would further enhance the utility of models. Coil positioning could become more accurate and robust with the development of advanced tracker-free stereotaxy and robotic coil holders.

It would also be desirable that TMS devices produce less noise and scalp sensation. More effective, electronically switchable sham coils would facilitate appropriate control conditions in studies. TMS has been integrated with the majority of neuroimaging modalities, although further technical advancements such as enhanced artifact reduction and subtraction would be welcome. Finally, the implementation of these promising technological developments in commercial products is an important step to enable advances in TMS applications.

References

- Agudelo-Toro, A. & Neef, A. (2013) Computationally efficient simulation of electrical activity at cell membranes interacting with self-generated and externally imposed electric fields. *Journal of Neural Engineering*, **10**, 026019.
- Aksöz, E., Aksöz, T., Bilge, S.S., İlkaya, F., Celik, S. & Diren, H.B. (2008) Antidepressant-like effects of echo-planar magnetic resonance imaging in mice determined using the forced swimming test. *Brain Research*, **1236**, 194–199.
- Antal, A., Kincses, T.Z., Nitsche, M.A. et al. (2002) Pulse configuration-dependent effects of repetitive transcranial magnetic stimulation on visual perception. *Neuroreport*, **13**, 2229–2233.
- Arai, N., Okabe, S., Furubayashi, T. et al. (2007) Differences in after-effect between monophasic and biphasic high-frequency rTMS of the human motor cortex. *Clinical Neurophysiology*, **118**, 2227–2233.
- Arai, N., Okabe, S., Furubayashi, T., Terao, Y., Yuasa, K. & Ugawa, Y. (2005) Comparison between short train, monophasic and biphasic repetitive transcranial magnetic stimulation (rTMS) of the human motor cortex. *Clinical Neurophysiology*, **116**, 605–613.
- Arana, A.B., Borckardt, J.J., Ricci, R. et al. (2008) Focal electrical stimulation as a sham control for repetitive transcranial magnetic stimulation: does it truly mimic the cutaneous sensation and pain of active prefrontal repetitive transcranial magnetic stimulation? *Brain Stimulation*, **1**, 44–51.
- Balslev, D., Braet, W., McAllister, C. & Miall, R.C. (2007) Inter-individual variability in optimal current direction for transcranial magnetic stimulation of the motor cortex. *Journal of Neuroscience Methods*, **162**, 309–313.
- Baltrušaitis, T., Robinson, P. & Morency, L. (2012) 3D Constrained Local Model for rigid and non-rigid facial tracking. *Proceedings of IEEE Conference on Computer Vision and Pattern Recognition*, 2610–2617.
- Barker, A.T., Garnham, C.W. & Freeston, I.L. (1991) Magnetic nerve stimulation: the effect of waveform on efficiency, determination of neural membrane time constants and the measurement of stimulator output. *Electroencephalography and Clinical Neurophysiology*, **43**, 227–237.
- Bersani, F.S., Minichino, A., Enticott, P.G. et al. (2013) Deep transcranial magnetic stimulation as a treatment for psychiatric disorders: a comprehensive review. *European Psychiatry*, **28**, 30–39.
- Bestmann, S., Baudewig, J. & Frahm, J. (2003) On the synchronization of transcranial magnetic stimulation and functional echo-planar imaging. *Journal of Magnetic Resonance Imaging*, **17**, 309–316.
- Bestmann, S., Ruff, C.C., Driver, J. & Blankenburg, F. (2008) Concurrent TMS and functional magnetic resonance imaging: methods and current advances. In: Wassermann, E.M., Epstein, C.M., Ziemann, U., Walsh, V., Paus, T. & Lisanby, S.H. (eds), *The Oxford Handbook of Transcranial Stimulation*. Oxford University Press, New York.
- Bettinardi, V., Presotto, L., Rapisarda, E., Picchio, M., Gianoli, L. & Gilardi, M.C. (2011) Physical performance of the new hybrid PETCT Discovery-690. *Medical Physics*, **38**, 5394–5411.
- Bijsterbosch, J.D., Barker, A.T., Lee, K.H. & Woodruff, P.W. (2012) Where does transcranial magnetic stimulation (TMS) stimulate? Modelling of induced field maps for some common cortical and cerebellar targets. *Medical and Biological Engineering and Computing*, **50**, 671–681.
- Bohning, D.E., Denslow, S., Bohning, P.A., Lomarev, M.P. & George, M.S. (2003a) Interleaving fMRI and rTMS. *Supplements to Clinical Neurophysiology*, **56**, 42–54.
- Bohning, D.E., Denslow, S., Bohning, P.A., Walker, J.A. & George, M.S. (2003b) A TMS coil positioning/holding system for MR image-guided TMS interleaved with fMRI. *Clinical Neurophysiology*, **114**, 2210–2219.
- Bohning, D.E., Shastri, A., Nahas, Z. et al. (1998) Echoplanar BOLD fMRI of brain activation induced by concurrent transcranial magnetic stimulation. *Investigative Radiology*, **33**, 336–340.
- Bonato, C., Miniussi, C. & Rossini, P.M. (2006) Transcranial magnetic stimulation and cortical evoked potentials: a TMS/EEG co-registration study. *Clinical Neurophysiology*, **117**, 1699–1707.
- Borckardt, J.J., Smith, A.R., Hutcheson, K. et al. (2006) Reducing pain and unpleasantness during repetitive transcranial magnetic stimulation. *Journal of ECT*, **22**, 259–264.
- Bowsher, K. & Eydelman, M.B. (2012) 510(k) summary K112881, nexstim navigational brainstimulation (NBS) system 4 and NBS system 4 with NEXSPEECH. In: Administration, U. F. A. D. (ed.). Silver Spring, MD.
- Brasil-Neto, J.P., Cohen, L.G., Panizza, M., Nilsson, J., Roth, B.J. & Hallett, M. (1992) Optimal focal transcranial magnetic activation of the human motor cortex: effects of coil orientation, shape of the induced current pulse, and stimulus intensity. *Jornal of Clinical Neurophysiology*, **9**, 132–136.

- Bungert, A., Chambers, C.D., Phillips, M. & Evans, C.J. (2012) Reducing image artefacts in concurrent TMS/fMRI by passive shimming. *Neuroimage*, **59**, 2167–2174.
- Cadwell, J. (1991) Optimizing magnetic stimulator design. *Electroencephalography and Clinical Neurophysiology*, **43**, 238–48.
- Carlezon, W.A.J., Rohan, M.L., Mague, S.D. et al. (2005) Antidepressant-like effects of cranial stimulation within a low-energy magnetic field in rats. *Biological Psychiatry*, **57**, 571–576.
- Catana, C., Drzezga, A., Heiss, W.D. & Rosen, B.R. (2012) PET/MRI for neurologic applications. *Journal of Nuclear Medicine*, **53**, 1916–1925.
- Chung, S.-H., Andersen, O.S. & Krishnamurthy, V. (2007) *Biological Membrane Ion Channels: Dynamics, Structure, and Applications*. Springer, New York.
- Claus, D., Murray, N.M., Spitzer, A. & Flugel, D. (1990) The influence of stimulus type on the magnetic excitation of nerve structures. *Electroencephalography and Clinical Neurophysiology*, **75**, 342–349.
- Cohen, D. & Cuffin, B.N. (1991) Developing a more focal magnetic stimulator. Part I: Some basic principles. *Journal of Clinical Neurophysiology*, **8**, 102–111.
- Corthout, E., Barker, A.T. & Cowey, A. (2001) Transcranial magnetic stimulation. Which part of the current waveform causes the stimulation? *Experimental Brain Research*, **141**, 128–132.
- Crowther, L.J., Marketos, P., Williams, P.I., Melikhov, Y., Jiles, D.C. & Starzewski, J.H. (2011) Transcranial magnetic stimulation: improved coil design for deep brain investigation. *Journal of Applied Physics*, **109**, 07B314.
- Crowther, L.J., Porzig, K., Hadimani, R.L., Brauer, H. & Jiles, D.C. (2012) Calculation of Lorentz forces on coils for transcranial magnetic stimulation during magnetic resonance imaging. *IEEE Transactions on Magnetics*, **48**, 4058–4061.
- Davey, K. & Epstein, C.M. (2000) Magnetic stimulation coil and circuit design. *IEEE Transaction on Biomedical Engineering*, **47**, 1493–1499.
- Davey, K.R. (2002). *Sham for transcranial magnetic stimulator*. US patent 6,491,620 B1.
- Davey, K.R. & Riehl, M.E. (2006) Suppressing the surface field during transcranial magnetic stimulation. *IEEE Transaction on Biomedical Engineering*, **53**, 190–194.
- Day, B.L., Dressler, D., Maertens De Noordhout, A. et al. (1989) Electric and magnetic stimulation of human motor cortex: surface EMG and single motor unit responses. *Journal of Physiology*, **412**, 449–473.
- De Geeter, N., Crevecoeur, G., Dupré, L., Van Hecke, W. & Leemans, A. (2012) A DTI-based model for TMS using the independent impedance method with frequency-dependent tissue parameters. *Physics in Medicine and Biology*, **57**, 2169–2188.
- Deng, Z.-D., Lisanby, S.H. & Peterchev, A.V. (2013) Electric field depth–focality tradeoff in transcranial magnetic stimulation: simulation comparison of 50 coil designs. *Brain Stimulation*, **6**, 1–13.
- Deng, Z.-D. & Peterchev, A.V. (2011) Transcranial magnetic stimulation coil with electronically switchable active and sham modes. Proceedings of Conference of IEEE Engineering in Medicine and Biology Society, 1993–1996.
- Deng, Z.-D., Lisanby, S.H. & Peterchev, A.V. (2014) Coil design considerations for deep transcranial magnetic stimulation. *Clinical Neurophysiology*, **125**, 1202–1212.
- Di Lazzaro, V., Profice, P., Ranieri, F. et al. (2012) I-wave origin and modulation. *Brain Stimulation*, **5**, 512–525.
- Dmochowski, J.P., Datta, A., Bikson, M., Su, Y. & Parra, L.C. (2011) Optimized multi-electrode stimulation increases focality and intensity at target. *Journal of Neural Engineering*, **8**, 046011.
- Drevets, W.C., Frank, E., Price, J.C. et al. (1999) PET imaging of serotonin 1A receptor binding in depression. *Biological Psychiatry*, **46**, 1375–1387.
- Edgley, S.A., Eyre, J.A., Lemon, R.N. & Miller, S. (1997) Comparison of activation of corticospinal neurons and spinal motor neurons by magnetic and electrical transcranial stimulation in the lumbosacral cord of the anaesthetized monkey. *Brain*, **120** (Pt 5), 839–853.
- Emrich, D., Fischer, A., Altenhofer, C. et al. (2012) Muscle force development after low-frequency magnetic burst stimulation in dogs. *Muscle and Nerve*, **46**, 954–956.
- Epstein, C.M. (2008) A six-pound battery-powered portable transcranial magnetic stimulator. *Brain Stimulation*, **1**, 128–130.
- Epstein, C.M. & Davey, K.R. (2002) Iron-core coils for transcranial magnetic stimulation. *Journal of Clinical Neurophysiology*, **19**, 376–381.
- Esser, S.K., Hill, S.L. & Tononi, G. (2005) Modeling the effects of transcranial magnetic stimulation on cortical circuits. *Journal of Neurophysiology*, **94**, 622–639.

- Farde, L., Hall, H., Ehrin, E. & Sedvall, G. (1986) Quantitative analysis of D2 dopamine receptor binding in the living human brain by PET. *Science*, **231**, 258–261.
- Geddes, L.A. (1987) Optimal stimulus duration for extracranial cortical stimulation. *Neurosurgery*, **20**, 94–99.
- Goetz, S.M., Herzog, H.G., Gattinger, N. & Gleich, B. (2011) Comparison of coil designs for peripheral magnetic muscle stimulation. *Journal of Neural Engineering*, **8**, 056007.
- Goetz, S.M., Luber, B., Lisanby, S.H. & Peterchev, A.V. (2014) A novel model incorporating two variability sources for describing motor evoked potentials. *Brain Stimulation*, **7**, 541–552.
- Goetz, S.M., Pfaffl, M., Huber, J. et al. (2012a) Circuit topology and control principle for a first magnetic stimulator with fully controllable waveform. Proceedings of Conference of IEEE Engineering in Medicine and Biology Society, 4700–4703.
- Goetz, S.M., Truong, C.N., Gerhofer, M.G., Peterchev, A.V., Herzog, H.-G. & Weyh, T. (2013) Analysis and Optimization of Pulse Dynamics for Magnetic Stimulation. *PLoS One*, **8**, e55771.
- Goetz, S.M., Truong, N.C., Gerhofer, M.G. et al. (2012b). Optimization of magnetic neurostimulation waveforms for minimum power loss. Proceedings of Conference of IEEE Engineering in Medicine and Biological Society, 4652–4655.
- Hernandez-Garcia, L., Hall, T., Gomez, L. & Michielssen, E. (2010) A numerically optimized active shield for improved transcranial magnetic stimulation targeting. *Brain Stimulation*, **3**, 218–225.
- Hoeft, F., Wu, D.A., Hernandez, A., Glover, G.H. & Shimojo, S. (2008) Electronically switchable sham transcranial magnetic stimulation (TMS) system. *PLoS One*, **3**, e1923.
- Hosono, Y., Urushihara, R., Harada, M. et al. (2008) Comparison of monophasic versus biphasic stimulation in rTMS over premotor cortex: SEP and SPECT studies. *Clinical Neurophysiology*, **119**, 2538–2545.
- Hovey, C. & Jalinous, R. (2006). The guide to magnetic stimulation. Available: <http://www.icts.uci.edu/neuroimaging/GuidetoMagneticStimulation2008.pdf> (accessed 17 November, 2011).
- Hsu, K.H. & Durand, D.M. (2001) A 3-D differential coil design for localized magnetic stimulation. *IEEE Transactions on Biomedical Engineering*, **48**, 1162–1168.
- Hutton, B.F. (2010) New SPECT technology: potential and challenges. *European Journal of Nuclear Medicine and Molecular Imaging*, **37**, 1883–1886.
- Ilmoniemi, R.J. & Kičić, D. (2010) Methodology for combined TMS and EEG. *Brain Topography*, **22**, 233–248.
- Ilmoniemi, R.J., Virtanen, J., Ruohonen, J. et al. (1997) Neuronal responses to magnetic stimulation reveal cortical reactivity and connectivity. *Neuroreport*, **8**, 3537–3540.
- Ives, J.R., Rotenberg, A., Poma, R., Thut, G. & Pascual-Leone, A. (2006) Electroencephalographic recording during transcranial magnetic stimulation in humans and animals. *Clinical Neurophysiology*, **117**, 1870–1875.
- Jalinous, R. (1991) Technical and practical aspects of magnetic nerve stimulation. *Journal of Clinical Neurophysiology*, **8**, 10–25.
- Judenhofer, M.S., Wehrle, H.F., Newport, D.F. et al. (2008) Simultaneous PET-MRI: a new approach for functional and morphological imaging. *Nature Medicine*, **14**, 459–465.
- Kammer, T., Beck, S., Thielbacher, A., Laubis-Herrmann, U. & Topka, H. (2001) Motor thresholds in humans: a transcranial magnetic stimulation study comparing different pulse waveforms, current directions and stimulator types. *Clinical Neurophysiology*, **112**, 250–258.
- Kammer, T., Vorwerg, M. & Herrnberger, B. (2007) Anisotropy in the visual cortex investigated by neuronavigated transcranial magnetic stimulation. *Neuroimage*, **36**, 313–321.
- Kantelhardt, S.R., Fadini, T., Finke, M. et al. (2010) Robot-assisted image-guided transcranial magnetic stimulation for somatotopic mapping of the motor cortex: a clinical pilot study. *Acta Neurochir (Wien)*, **152**, 333–343.
- Kato, A., Yoshimine, T., Hayakawa, T. et al. (1991) A frameless, armless navigational system for computer-assisted neurosurgery. Technical note. *Journal of Neurosurgery*, **74**, 845–849.
- Khadem, R., Yeh, C.C., Sadeghi-Tehrani, M. et al. (2000) Comparative tracking error analysis of five different optical tracking systems. *Computer Aided Surgery*, **5**, 98–107.
- Kim, D.-H., Georgiou, G.E. & Won, C. (2006) Improved field localization in transcranial magnetic stimulation of the brain with the utilization of a conductive shield plate in the stimulator. *IEEE Transaction on Biomedical Engineering*, **53**, 720–725.
- Kimbell, T.A., Dunn, R.T., George, M.S. et al. (2002) Left prefrontal-repetitive transcranial magnetic stimulation (rTMS) and regional cerebral glucose metabolism in normal volunteers. *Psychiatry Research*, **115**, 101–113.

- Knäulein, R. & Weyh, T. (1996) Minimization of energy stored in the magnetic field of air coils for medical application. 3rd International Workshop on Electric and Magnetic Fields, Liege. 477–482.
- Korhonen, R.J., Hernandez-Pavon, J.C., Metsomaa, J., Mäki, H., Ilmoniemi, R.J. & Sarvas, J. (2011) Removal of large muscle artifacts from transcranial magnetic stimulation-evoked EEG by independent component analysis. *Medical and Biological Engineering and Computing*, **49**, 397–407.
- Lancaster, J.L., Narayana, S., Wenzel, D., Luckemeyer, J., Roby, J. & Fox, P. (2004) Evaluation of an image-guided, robotically positioned transcranial magnetic stimulation system. *Human Brain Mapping*, **22**, 329–340.
- Lapicque, L. (1907) Recherches quantitatives sur l'excitation électrique des nerfs traitée comme une polarization. *Journal de Physiologie et de Pathologie Générale*, **9**, 620–635.
- Lisanby, S.H., Gutman, D., Luber, B., Schroeder, C. & Sackeim, H.A. (2001) Sham TMS: intracerebral measurement of the induced electrical field and the induction of motor-evoked potentials. *Biological Psychiatry*, **49**, 460–463.
- Lisanby, S.H. & Peterchev, A.V. (2007) Magnetic seizure therapy for the treatment of depression. In: Marcolin, M.A. & Padberg, F. (eds), *Transcranial Brain Stimulation for Treatment in Mental Disorders*. Karger Publishers, New York.
- Litvak, V., Komssi, S., Scherg, M. et al. (2007) Artifact correction and source analysis of early electroencephalographic responses evoked by transcranial magnetic stimulation over primary motor cortex. *NeuroImage*, **37**, 56–70.
- Loo, C.K., Taylor, J.L., Gandevia, S.C., Mcdarmont, B.N., Mitchell, P.B. & Sachdev, P.S. (2000) Transcranial magnetic stimulation (TMS) in controlled treatment studies: are some “sham” forms active? *Biological Psychiatry*, **47**, 325–331.
- Lorenzen, H.W. & Weyh, T. (1992) Practical Application of the Summation Method for 3-D Static Magnetic-Field Calculation of a Setup of Conductive and Ferromagnetic Material. *IEEE Transaction on Magnetics*, **28**, 1481–1484.
- Maccabee, P.J., Nagarajan, S.S., Amassian, V.E. et al. (1998) Influence of pulse sequence, polarity and amplitude on magnetic stimulation of human and porcine peripheral nerve. *Journal of Physiology*, **513**, 571–585.
- Maccaferri, G. & Lacaille, J.C. (2003) Interneuron Diversity series: Hippocampal interneuron classifications—making things as simple as possible, not simpler. *Trends in Neurosciences*, **26**, 564–571.
- Markram, H., Toledo-Rodriguez, M., Wang, Y., Gupta, A., Silberberg, G. & Wu, C. (2004) Interneurons of the neocortical inhibitory system. *Nature Review Neuroscience*, **5**, 793–807.
- Mc Robbie, D. (1985) Design and Instrumentation of a Magnetic Nerve Stimulator. *Journal of Physics E-Scientific Instruments*, **18**, 74–78.
- Mennemeier, M.S., Triggs, W.J., Chelette, K.C., Woods, A.J., Kimbrell, T.A. & Dornhoffer, J.L. (2009) Sham transcranial magnetic stimulation using electrical stimulation of the scalp. *Brain Stimulation*, **2**, 169–173.
- Moisa, M., Pohmann, R., Ewald, L. & Thielscher, A. (2009) New coil positioning method for interleaved transcranial magnetic stimulation (TMS)/functional MRI (fMRI) and its validation in a motor cortex study. *Journal of Magnetic Resonance Imaging*, **29**, 189–197.
- Morbidì, F., Garulli, A., Prattichizzo, D., Rizzo, C., Manganotti, P. & Rossi, S. (2007) Off-line removal of TMS-induced artifacts on human electroencephalography by Kalman filter. *Journal of Neuroscience Methods*, **162**, 293–302.
- Murphy-Chutorian, E. & Trivedi, M.M. (2009) Head Pose Estimation in Computer Vision: A Survey. *IEEE Transactions on Pattern Analysis and Machine Intelligence*, **31**, 607–626.
- Nahas, Z., Teneback, C.C., Kozel, A. et al. (2001) Brain effects of TMS delivered over prefrontal cortex in depressed adults: role of stimulation frequency and coil-cortex distance. *Journal of Neuropsychiatry and Clinical Neuroscience*, **13**, 459–470.
- Nasi, T., Maki, H., Kotilahti, K., Nissila, I., Haapalahti, P. & Ilmoniemi, R.J. (2011) Magnetic-stimulation-related physiological artifacts in hemodynamic near-infrared spectroscopy signals. *PLoS One*, **6**, e24002.
- Niehaus, L., Meyer, B.U. & Weyh, T. (2000) Influence of pulse configuration and direction of coil current on excitatory effects of magnetic motor cortex and nerve stimulation. *Clinical Neurophysiology*, **111**, 75–80.
- Okabe, S., Hanajima, R., Ohnishi, T. et al. (2003a) Functional connectivity revealed by single-photon emission computed tomography (SPECT) during repetitive transcranial magnetic stimulation (rTMS) of the motor cortex. *Clinical Neurophysiology*, **114**, 450–457.
- Okabe, S., Ugawa, Y., Kanazawa, I. & Effectiveness of Rtms on Parkinson's Disease Study Group (2003b) 0.2-Hz repetitive transcranial magnetic stimulation has no add-on effects as compared to a realistic sham stimulation in Parkinson's disease. *Movement Disorders*, **18**, 382–388.

- Opitz, A., Legon, W., Rowlands, A., Bickel, W.K., Paulus, W. & Tyler, W.J. (2013) Physiological observations validate finite element models for estimating subject-specific electric field distributions induced by transcranial magnetic stimulation of the human motor cortex. *NeuroImage*, **81**, 253–264.
- Opitz, A., Windhoff, M., Heidemann, R.M., Turner, R. & Thielscher, A. (2011) How the brain tissue shapes the electric field induced by transcranial magnetic stimulation. *NeuroImage*, **58**, 849–859.
- Orth, M. & Rothwell, J.C. (2004) The cortical silent period: intrinsic variability and relation to the waveform of the transcranial magnetic stimulation pulse. *Clinical Neurophysiology*, **115**, 1076–1082.
- Peterchev, A.V., D'Ostilio, K., Rothwell, J.C. & Murphy, D.L. (2014) Controllable pulse parameter transcranial magnetic stimulator with enhanced circuit topology and pulse shaping. *Journal of Neural Engineering*, **11**, 056023.
- Peterchev, A.V., Goetz, S.M., Westin, G.G., Luber, B. & Lisanby, S.H. (2013) Pulse width dependence of motor threshold and input-output curve characterized with controllable pulse parameter transcranial magnetic stimulation. *Clinical Neurophysiology*, **124**, 1364–1372.
- Peterchev, A.V., Jalinous, R. & Lisanby, S.H. (2008) A transcranial magnetic stimulator inducing near-rectangular pulses with controllable pulse width (cTMS). *IEEE Transaction on Biomedical Engineering*, **55**, 257–266.
- Peterchev, A.V., Murphy, D.L. & Lisanby, S.H. (2011) Repetitive transcranial magnetic stimulator with controllable pulse parameters. *Journal of Neural Engineering*, **8**, 036016.
- Peterchev, A.V., Wagner, T.A., Miranda, P.C. et al. (2012) Fundamentals of transcranial electric and magnetic stimulation dose: definition, selection, and reporting practices. *Brain Stimulation*, **5**, 435–453.
- Ren, C., Tarjan, P.P. & Popovic, D.B. (1995) A novel electric design for electromagnetic stimulation—the Slinky coil. *IEEE Transaction on Biomedical Engineering*, **42**, 918–925.
- Roberts, D.W., Strohbehn, J.W., Hatch, J.F., Murray, W. & Kettenberger, H. (1986) A frameless stereotaxic integration of computerized tomographic imaging and the operating microscope. *Journal of Neurosurgery*, **65**, 545–549.
- Rohan, M., Parow, A., Stoll, A.L. et al. (2004) Low-field magnetic stimulation in bipolar depression using an MRI-based stimulator. *American Journal of Psychiatry*, **161**, 93–98.
- Rokni-Yazdi, H., Sotoudeh, H., Akhondzadeh, S., Sotoudeh, E., Asadi, H. & Shakiba, M. (2007) Antidepressant-like effect of magnetic resonance imaging-based stimulation in mice. *Progress of Neuropsychopharmacology and Biological Psychiatry*, **31**, 503–509.
- Rossi, S., Ferro, M., Cincotta, M. et al. (2007) A real electro-magnetic placebo (REMP) device for sham transcranial magnetic stimulation (TMS). *Clinical Neurophysiology*, **118**, 709–716.
- Rossi, S., Hallett, M., Rossini, P.M., Pascual-Leone, A. & Safety of Tms Consensus Group (2009) Safety, ethical considerations, and application guidelines for the use of transcranial magnetic stimulation in clinical practice and research. *Clinical Neurophysiology*, **120**, 2008–2039.
- Roth, B.J., Pascual-Leone, A., Cohen, L.G. & Hallett, M. (1992) The heating of metal electrodes during rapid-rate magnetic stimulation: a possible safety hazard. *Electroencephalography and Clinical Neurophysiology*, **85**, 116–123.
- Roth, B.J., Turner, R., Cohen, L.G. & Hallett, M. (1990) New coil design for magnetic stimulation with improved focality. *Movement Disorders*, **5**, S32.
- Roth, Y., Pell, G.S. & Zangen, A. (2013) Commentary on: Deng et al., Electric field depth–focality tradeoff in transcranial magnetic stimulation: simulation comparison of 50 coil designs. *Brain Stimulation*, **6**, 14–15.
- Roth, Y. & Zangen, A. (2006) Transcranial magnetic stimulation of deep brain regions. In: Bronzino, J.D. (ed), *Biomedical Engineering Fundamentals*, 3rd edn. CRC Press/Taylor & Francis, Boca Raton, FL.
- Rothkegel, H., Sommer, M., Paulus, W. & Lang, N. (2010) Impact of pulse duration in single pulse TMS. *Clinical Neurophysiology*, **121**, 1915–1921.
- Ruohonen, J. & Ilmoniemi, R. (1998) Focusing and targeting of magnetic brain stimulation using multiple coils. *Medical and Biological Engineering and Computing*, **36**, 297–301.
- Ruohonen, J. & Karhu, J. (2010) Navigated transcranial magnetic stimulation. *Neurophysiology Clinical*, **40**, 7–17.
- Ruohonen, J., Ollikainen, M., Nikouline, V., Virtanen, J. & Ilmoniemi, R.J. (2000) Coil design for real and sham transcranial magnetic stimulation. *IEEE Transactions on Biomedical Engineering*, **47**, 145–148.
- Schmid, M., Weyh, T. & Meyer, B.U. (1993) Development, optimization and evaluation of new instruments for magnetomotor stimulation of nerve fibers. *Biomedical Technology/Biomedical Engineering*, **38**, 317–324.
- Shastri, A., George, M.S. & Bohning, D.E. (1999) Performance of a system for interleaving transcranial magnetic stimulation with steady-state magnetic resonance imaging. *Electroencephalography and Clinical Neurophysiology*, **51**, 55–64.

- Sibon, I., Strafella, A.P., Gravel, P. et al. (2007) Acute prefrontal cortex TMS in healthy volunteers: effects on brain ¹¹C-alphaMtrp trapping. *Neuroimage*, **34**, 1658–1664.
- Siebner, H., Weyh, T., Ziegler, S. et al. (1999) Electromagnetic shielding is advisable in studies combining cortical magnetic stimulation and PET. *Neuroimage*, **9**, S170–S170.
- Siebner, H.R., Bergmann, T.O., Bestmann, S. et al. (2009) Consensus paper: combining transcranial stimulation with neuroimaging. *Brain Stimulation*, **2**, 58–80.
- Siebner, H.R., Takano, B., Peinemann, A., Schwaiger, M., Conrad, B. & Drzezga, A. (2001) Continuous transcranial magnetic stimulation during positron emission tomography: a suitable tool for imaging regional excitability of the human cortex. *Neuroimage*, **14**, 883–890.
- Skinner, F. & Saraga, F. (2010) *Single neuron models: Interneurons. Hippocampal Microcircuits*. Springer, New York.
- Sommer, J., Jansen, A., Drager, B. et al. (2006a) Transcranial magnetic stimulation--a sandwich coil design for a better sham. *Clinical Neurophysiology*, **117**, 440–446.
- Sommer, M., Alfaro, A., Rummel, M. et al. (2006b) Half sine, monophasic and biphasic transcranial magnetic stimulation of the human motor cortex. *Clinical Neurophysiology*, **117**, 838–844.
- Sommer, M., Lang, N., Tergau, F. & Paulus, W. (2002) Neuronal tissue polarization induced by repetitive transcranial magnetic stimulation? *Neuroreport*, **13**, 809–811.
- Sommer, M., Norden, C., Schmack, L., Rothkegel, H., Lang, N. & Paulus, W. (2013) Opposite optimal current flow directions for induction of neuroplasticity and excitation threshold in the human motor cortex. *Brain Stimulation*, **6**, 363–370.
- Strafella, A.P., Paus, T., Fraraccio, M. & Dagher, A. (2003) Striatal dopamine release induced by repetitive transcranial magnetic stimulation of the human motor cortex. *Brain*, **126**, 2609–2615.
- Suehiro, M., Scheffel, U., Dannals, R.F., Ravert, H.T., Ricaurte, G.A. & Wagner, H.N. Jr. (1993) A PET radiotracer for studying serotonin uptake sites: carbon-11-McN-5652Z. *Journal of Nuclear Medicine*, **34**, 120–127.
- Takano, B., Drzezga, A., Peller, M. et al. (2004) Short-term modulation of regional excitability and blood flow in human motor cortex following rapid-rate transcranial magnetic stimulation. *Neuroimage*, **23**, 849–859.
- Taylor, J.L. & Loo, C.K. (2007) Stimulus waveform influences the efficacy of repetitive transcranial magnetic stimulation. *Journal of Affective Disorders*, **97**, 271–276.
- Tebo, S.A., Leopold, D.A., Long, D.M., Zinreich, S.J. & Kennedy, D.W. (1996) An optical 3D digitizer for frameless stereotactic surgery. *Computer Graphics and Applications, IEEE*, **16**, 55–64.
- Thielscher, A., Opitz, A. & Windhoff, M. (2011) Impact of the gyral geometry on the electric field induced by transcranial magnetic stimulation. *Neuroimage*, **54**, 234–243.
- Tings, T., Lang, N., Tergau, F., Paulus, W. & Sommer, M. (2005) Orientation-specific fast rTMS maximizes corticospinal inhibition and facilitation. *Experimental Brain Research*, **164**, 323–333.
- Toschi, N., Keck, M.E., Welt, T. & Guerrisi, M. (2012) Quantifying uncertainty in transcranial magnetic stimulation -- a high resolution simulation study in ICBM space. Proceedings of Conference of IEEE Engineering Medical Biology Society, 1218–1221.
- Toschi, N., Welt, T., Guerrisi, M. & Keck, M.E. (2009) Transcranial magnetic stimulation in heterogeneous brain tissue: clinical impact on focality, reproducibility and true sham stimulation. *Journal of Psychiatric Research*, **43**, 255–264.
- Vaziri-Bozorg, S.M., Ghasemi-Esfe, A.R., Khalilzadeh, O. et al. (2012) Antidepressant effects of magnetic resonance imaging-based stimulation on major depressive disorder: a double-blind randomized clinical trial. *Brain Imaging Behavior*, **6**, 70–76.
- Virtanen, J., Ruohonen, J., Naatanen, R. & Ilmoniemi, R.J. (1999) Instrumentation for the measurement of electric brain responses to transcranial magnetic stimulation. *Medicine and Biological Engineering and Computing*, **37**, 322–326.
- Volkow, N.D., Tomasi, D., Wang, G.J. et al. (2010) Effects of low-field magnetic stimulation on brain glucose metabolism. *Neuroimage*, **51**, 623–628.
- Wada, S., Kubota, H., Maita, S. et al. (1996) Effects of stimulus waveform on magnetic nerve stimulation. *Japanese Journal of Applied Physics*, **1** (35), 1983–1988.
- Wassermann, E.M., Wang, B., Zeffiro, T.A. et al. (1996) Locating the motor cortex on the MRI with transcranial magnetic stimulation and PET. *Neuroimage*, **3**, 1–9.
- Weiskopf, N., Josephs, O., Ruff, C.C. et al. (2009) Image artifacts in concurrent transcranial magnetic stimulation (TMS) and fMRI caused by leakage currents: modeling and compensation. *Journal of Magnetic Resonance Imaging*, **29**, 1211–1217.

- Weyh, T., Wendicke, K., Mentschel, C., Zantow, H. & Siebner, H.R. (2005) Marked differences in the thermal characteristics of figure-of-eight shaped coils used for repetitive transcranial magnetic stimulation. *Clinical Neurophysiology*, **116**, 1477–1486.
- Windhoff, M., Opitz, A. & Thielscher, A. (2013) Electric field calculations in brain stimulation based on finite elements: An optimized processing pipeline for the generation and usage of accurate individual head models. *Human Brain Mapping*, **34**, 923–935.
- Wolf, M., Ferrari, M. & Quaresima, V. (2007) Progress of near-infrared spectroscopy and topography for brain and muscle clinical applications. *Journal of Biomedical Optics*, **12**, 062104.
- Yang, W., Gupta, M., Song, Z. et al. (2005) High resolution tracking of non-rigid 3D motion of densely sampled data using harmonic maps. Proceedings of IEEE International Conference on Computer Vision, **1**, 388–395.
- Zorn, L., Renaud, P., Bayle, B. et al. (2012) Design and evaluation of a robotic system for transcranial magnetic stimulation. *IEEE Transaction on Biomedical Engineering*, **59**, 805–815.